



# Recent Developments in Suspension Plasma Sprayed Titanium Oxide and Hydroxyapatite Coatings

R. Jaworski, L. Pawlowski, C. Pierlot, F. Roudet, S. Kozerski, and F. Petit

(Submitted July 23, 2009; in revised form August 20, 2009)

The paper aims at reviewing of the recent studies related to the development of suspension plasma sprayed  $\text{TiO}_2$  and  $\text{Ca}_5(\text{PO}_4)_3\text{OH}$  (hydroxyapatite, HA) coatings as well as their multilayer composites obtained onto stainless steel, titanium and aluminum substrates. The total thickness of the coatings was in the range 10 to 150  $\mu\text{m}$ . The suspensions on the base of distilled water, ethanol and their mixtures were formulated with the use of fine commercial  $\text{TiO}_2$  pigment crystallized as rutile and HA milled from commercial spray-dried powder or synthesized from calcium nitrate and ammonium phosphate in an optimized reaction. The powder was crystallized as hydroxyapatite. Pneumatic and peristaltic pump liquid feeders were applied. The injection of suspension to the plasma jet was studied carefully with the use of an atomizer injector or a continuous stream one. The injectors were placed outside or inside of the anode-nozzle of the SG-100 plasma torch. The stream of liquid was tested under angle right or slightly backwards with regard to the torch axis. The sprayed deposits were submitted to the phase analysis by the use of x-ray diffraction. The content of anatase and rutile was calculated in the titanium oxide deposits as well as the content of the decomposition phases in the hydroxyapatite ones. The micro-Raman spectroscopy was used to visualize the area of appearance of some phases. Scratch test enabled to characterize the adhesion of the deposits, their microhardness and friction coefficient. The electric properties including electron emission, impedance spectroscopy, and dielectric properties of some coatings were equally tested.

**Keywords** hydroxyapatite, suspension plasma spraying, titanium oxide

## 1. Introduction

Suspension and solution thermal spraying are the “hot topics” in the coatings’ technology and literature brings continuously new results related to the improvement in deposition technology, reviewed in Ref 1, and to the new,

possible applications of the coatings, reviewed in Ref 2. The ceramic coatings deposition seems to be particularly often studied. Titanium oxide and hydroxyapatite are the typical examples of this interest.

Titanium oxide films and coatings have been studied recently because of their interesting physical, chemical and electrical properties. Such application of coatings as hydrogen and oxygen sensors (Ref 3, 4), self-cleaning and photocatalytic surfaces, useful in degrading organic pollutants (Ref 5) but also electron emitters for light emitting devices (Ref 6, 7) have been considered. The  $\text{TiO}_2$  coatings have been synthesized by many methods including physical and chemical vapor deposition, sol-gel and more recently by electrophoretic deposition (Ref 8). Thermal spraying techniques have been frequently used to obtain thick titania coatings sprayed using coarse powder particles reviewed recently by Berger (Ref 9). Thin layers (10-30  $\mu\text{m}$ ) have been synthesized by injection water suspension of nanometric and submicrometer titania powder particles into high-velocity combustion flame (Ref 10) or plasma jet (Ref 11-13). The obtained deposits had characterized the following microstructural features, namely:

- morphology using scanning electron and optical microscopes;
- chemical composition using x-ray photoelectron spectroscopy;
- phase composition using x-ray diffraction method and Raman microscopy.

This article is an invited paper selected from presentations at the 2009 International Thermal Spray Conference and has been expanded from the original presentation. It is simultaneously published in *Expanding Thermal Spray Performance to New Markets and Applications: Proceedings of the 2009 International Thermal Spray Conference*, Las Vegas, Nevada, USA, May 4-7, 2009, Basil R. Marple, Margaret M. Hyland, Yuk-Chiu Lau, Chang-Jiu Li, Rogerio S. Lima, and Ghislain Montavon, Ed., ASM International, Materials Park, OH, 2009.

**R. Jaworski, L. Pawlowski, and C. Pierlot**, Ecole Nationale Supérieure de Chimie de Lille, BP 90108, 59650 Villeneuve d’Ascq, France; **F. Roudet**, University of Lille 1, Le Recueil, BP 179, 59653 Villeneuve d’Ascq, France; **S. Kozerski**, Wrocław University of Technology, 50-370 Wrocław, Poland; and **F. Petit**, Belgian Ceramic Research Centre, 7000 Mons, Belgium. Contact e-mail: lech.pawlowski@ensc-lille.fr.

Hydroxyapatite (HA, having chemical formula  $\text{Ca}_{10}(\text{PO}_4)_6(\text{OH})_2$ ) is a bioactive ceramics which owing to chemical composition and crystal structure similar to those of human bone can facilitate integration of prostheses into osseous tissue (Ref 14-16). The ceramics has been used to restore bone tissue and to decrease the negative consequence of surgical operation for many years. Because of its limited mechanical strength, HA is used as coating on surfaces of more resistant metallic prostheses made of, e.g., Ti-6Al-4V alloy (Ref 17). The environment rich of calcium and phosphate at the surface of prosthesis favors development of bone cells and enhances its adhesion to the bone (Ref 14). Atmospheric plasma spraying (APS) is the most widely applied method to deposit HA coating onto titanium alloy prostheses. The method consists of injection of ceramic particles into a high-temperature ( $>10,000$  K) and high-velocity ( $>800$  m/s) plasma jet (Ref 18). The high temperature provokes dehydration and decomposition of HA. The dehydration produces oxyapatite (OA,  $\text{Ca}_{10}(\text{PO}_4)_6\text{O}$ ) and/or oxyhydroxyapatite (OHA,  $\text{Ca}_{10}(\text{PO}_4)_6(\text{OH})_{2-x}\text{O}_x\text{V}_x$ ), in which V means vacancy. The decomposition, in turn, results in different calcium phosphate phases such as, e.g. calcium oxide (CaO),  $\alpha$ -tricalcium phosphate ( $\alpha$ -TCP,  $\alpha\text{-Ca}_3(\text{PO}_4)_2$ ),  $\beta$ -tricalcium phosphate ( $\beta$ -TCP,  $\beta\text{-Ca}_3(\text{PO}_4)_2$ ), tetracalcium phosphate (TTCP,  $\text{Ca}_4\text{P}_2\text{O}_9$ ) and/or the amorphous calcium phosphate (ACP). A spray particle impacting a surface, at plasma spraying using typical processing parameters, is composed of a solid core and liquid shell (Ref 19). Fast cooling of crystal phases in the solid core at impact results in conservation of high-temperature phases. The liquid shell is most probably transformed at impact into an amorphous phase. The fractions of HA, OA-OHA, TTCP,  $\alpha$ -TCP and ACP phases in sprayed coatings is the most important factor that determines their biological behavior, such as dissolution of the coating in vivo (Ref 20). Careful control of operational spray parameters may help in predicting the phase content in the coating (Ref 21).

## 2. Experimental

### 2.1 Suspensions Preparation

Two aqueous suspensions were prepared for spraying. Suspension was formulated with the use of rutile manufactured by Tioxide (R-TC90 of Huntsman Tioxide) by taking distilled water + 4 wt.% rutile + 0.3 wt.% dispersant. The characteristics of the pigment are presented in Ref 12. The dispersant was an aqueous solution of sodium polyacrylate (Hydropalat N, Congis). A commercial powder Tomita (Japan) was used for preparation of suspension HA. The initial powder characteristics are shown elsewhere (Ref 22). The powder was ball-milled using moliNEx system (Netsch, Germany) in ethanol for 8 h using zirconia balls. The suspension was then formulated with the use of tetra-sodium diphosphate (Table 1).

**Table 1 Composition of suspensions used in most of the deposition runs**

Components	Quantity
TiO <sub>2</sub> suspension	
Solid particles: TiO <sub>2</sub> Huntsman	10 wt.%
Dispersant: Hydropalat N	0.3 dwb%
HA suspension	
Solid particles: ball-milled HA	10 wt.%
Dispersant: tetra-sodium diphosphate	0.3 dwb%

dwb indicates the weight amount of dispersant on a dry weight basis of powder

**Table 2 Typical plasma spray parameters of suspension sprayed coatings**

Coating type	Working gases flow rate, slpm	Electric arc power, kW	Torch linear velocity, mm/s	Spray distance, cm
TiO <sub>2</sub> , HA and their multilayer composites	Ar-45 H <sub>2</sub> -5	30-40	200-500	6-12

### 2.2 Plasma Spraying

Stainless steel, aluminum and titanium plates having dimensions  $15 \times 15 \times 3$  mm were used as coatings substrates. They were alumina grit-blasted. The substrates were plasma sprayed using Praxair SG-100 torch mounted on the 5-axis ABB IRB-6 industrial robot. The typical spray parameters are collected in Table 2. The trajectory of torch at spraying of coatings is presented elsewhere (Ref 13). The geometries of atomizer and continuous stream suspension injectors to the plasma jet are shown in Fig. 1. The continuous stream injector was applied outside and inside anode-nozzle of the torch. The dimensions shown in the figure have varied throughout the experiments.

### 2.3 Powders and Coatings Characterization

Morphologies of powders and coatings were investigated using JSM 6060 microscope equipped with a detector of secondary electrons. The cross sections of coatings were prepared metallographically. The powders particles sizes were determined using Malvern Mastersizer X set up. XRD analyses were carried out using a diffractometer of Bruker model D8 using  $\text{CuK}_\alpha$  radiation. The crystal phases were identified with help of Diffrac<sup>plus</sup> EVA software. The software uses the database of International Centre of Diffraction Data JCPDS-ICDD. Micro-Raman spectroscopic investigations were carried out using Dilor-Jobin Yvon-Spex spectrometer of type LabRam, which uses HeNe laser (632.8 nm, 8 mW) as excitation source. The spot of the Raman analysis was equal approximately to 1  $\mu\text{m}$ . Coatings thicknesses were measured using tester of Mitutoyo model ASZ845 which has a precision of 1  $\mu\text{m}$ . Samples for measurements of electrical properties were

prepared by applying an electrode on the top of the coating. The electrode of Ag-rich paint was put on the centre of sample and had a diameter of 7 mm and aluminium substrate was the second one. The breakdown voltages were measured by applying on the top of coating a copper electrode with a size of about 5 mm. The electrode was pushed by spring to the sample. Voltage was applied using high-voltage power supply of Polon (Poland) model ZWN-41 and was measured using Metex M3860D voltmeter. The voltage was increased manually every 10 V until breakdown occurs. The breakdown voltage value corresponded typically to the current of a few microamperes. The current was measured using Metex M3610 amperemeter. The scratch tests were performed with a MicroCombiTester of CSM Instruments equipped with a Rockwell diamond indenter having a tip radius of 0.2 mm. As the coatings are very porous, the acoustic signal could not be used to the estimation of critical load,  $L_c$ . In the present work, the critical load was defined at the onset of the coating loss associated with a beginning of visibility of metallic substrate inside the scratch channel. This measurement was made with a help of optical microscope. The tester enabled also to find the friction coefficient at the critical load. The scratch hardness  $HS_L$  (Pa) was estimated following the specification of ASTM G171-03 norm:

$$HS_L = \frac{8 \cdot L}{\pi \cdot d^2} \quad (\text{Eq 1})$$

where  $L$  (N) is the applied normal force (the load of 30 N was selected) and  $d$  (m) is the corresponding scratch width. The scratch hardness is an indicator of coating

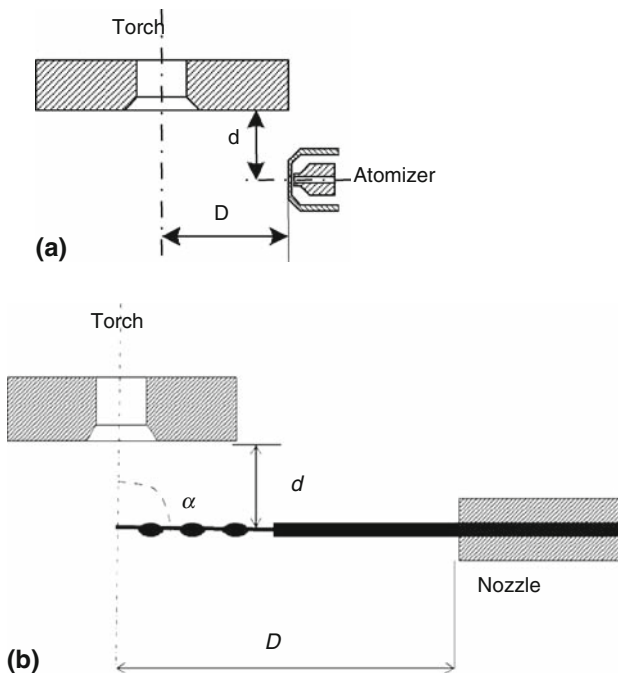


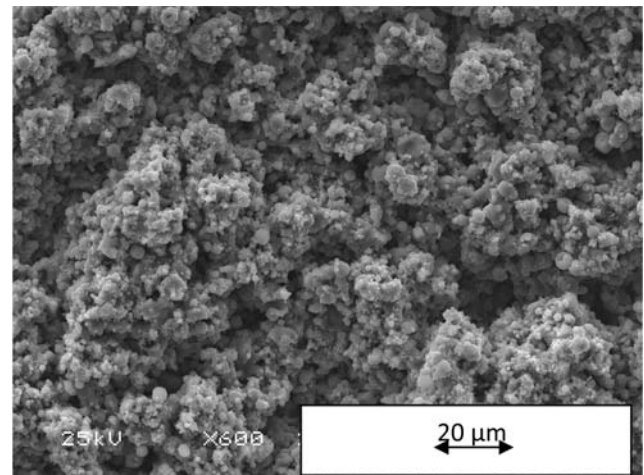
**Fig. 1** Injectors used in the experiments: (a) atomizer and (b) continuous stream injector

cohesion. The impedance spectroscopy measurements were carried out with impedance analyzer Solartron type SI 1260. The applied signal was 0.5 V in 100 Hz to 2 MHz frequency range. The temperature of the samples was automatically controlled in the range of 320 to 1020 K by computerized power supply device Agilent type E3632A.

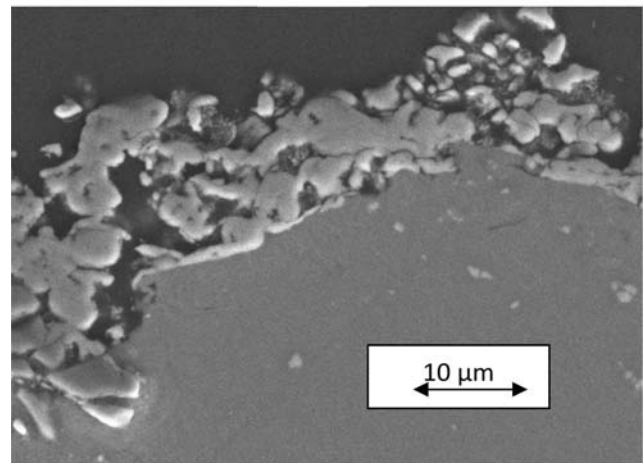
### 3. Results and Discussion

#### 3.1 $TiO_2$ Coatings

The morphology of  $TiO_2$  coating is shown in Fig. 2. The coatings sprayed using rutile have some agglomerates having typical size of a few tenths of micrometers (Fig. 2a) and small spherical particles which solidified before impact with previously deposited coating. The cross section of rutile sprayed coating confirms important porosity



(a)



(b)

**Fig. 2** SEM (secondary electrons) of the surface (a) and cross section (b) of the  $TiO_2$  coating suspension plasma sprayed using fine rutile pigment as solid phase and an atomizer injector. The spray distance was equal to 12 cm and detailed description of technology is shown elsewhere (Ref 21, 22)

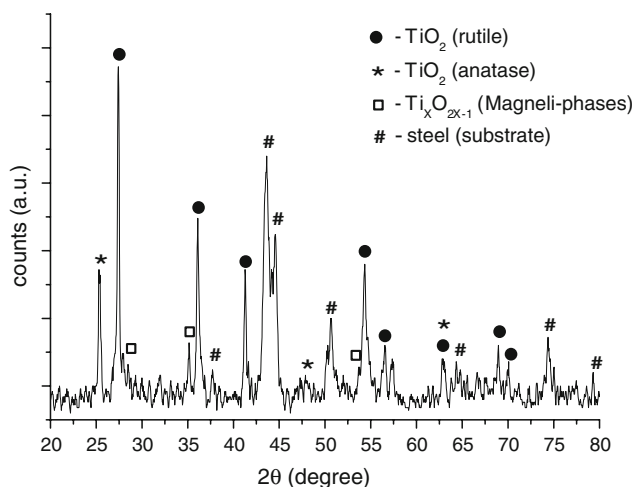


**Fig. 3** X-ray diffraction diagram of suspension plasma sprayed  $\text{TiO}_2$  coating (Ref 10)

of the rutile sprayed deposits (Fig. 2b). Typical XRD of suspension plasma sprayed  $\text{TiO}_2$  coating is shown in Fig. 3. XRD analysis shows multi-phase composition of the coating. The most intense peaks correspond to rutile, then come that of anatase and Magnéli phases shown elsewhere (Ref 12) and discussed extensively in Ref 7. The formation of the phases results from the loss of oxygen by  $\text{TiO}_2$ . Again, some peaks correspond to the substrate and there is a shift in direction of smaller angles for  $\text{TiO}_2$  peaks. The shift is equal to  $2\Theta = 0.370^\circ$  which indicates the tensile stresses in sprayed coating. The size of rutile grains was estimated to be 28–69 nm. The distribution of rutile and anatase phase has been made with the use of the micro-Raman microscopy and is shown in Fig. 4. There are the spots of pure anatase, pure rutile and mixed spots of the two phases. Unfortunately, the micro-Raman spectroscopy does not allow visualizing the spots corresponding to Magnéli phases. Thermoanalytic methods, such as thermogravimetric analysis (TGA) or differential thermal analysis (DTA), can be possibly useful in their identification. More details are presented in Ref 23. The formation of anatase depends on the operational spray parameters—mainly on spray distance. Its content varies from 9 to 15 wt.% and anatase crystal sizes vary from 80 to 105 nm (Ref 24). To understand the mechanism of anatase formation, it is necessary to look into the behavior of liquid droplets injected to the plasma jet. Knowing that the size of suspension delivery outlet is 700  $\mu\text{m}$  (see Fig. 1) and that the liquid is subsequently atomized, the sizes of droplets must have diameter ranging from a few tens to a few hundreds of micrometers. The droplets are accelerated in the plasma jet and, simultaneously, water boils and gets evaporated. The solid precursors inside any droplet get closer and may start to agglomerate by sintering in flight. The process can be compared to that of spray-drying described by Masters (Ref 25). However, the processes have the following significant differences:

- particularly hot heating medium (plasma jet);
- boiling of suspension liquid;

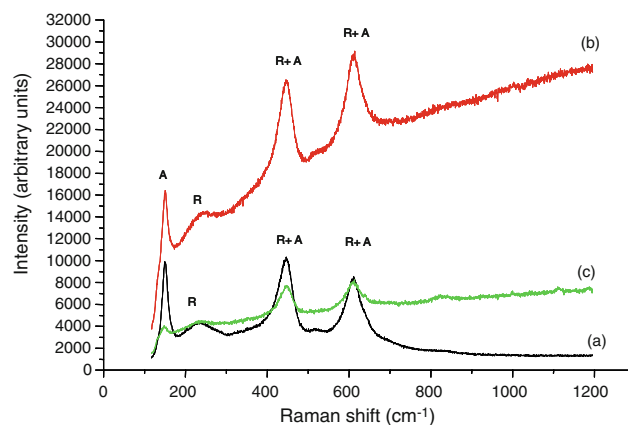
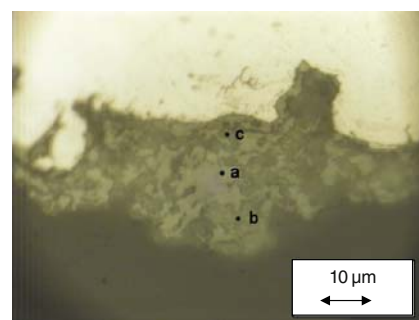


**Fig. 4** Micro-Raman analysis of a few spots in the cross section of suspension plasma sprayed  $\text{TiO}_2$  coating. A, spots of anatase; R, rutile (Ref 21)

- very short heating time (milliseconds instead of seconds); and
- missing of a binder in the liquid.

A part of small solids gets molten in the initial part of their trajectory. In fact, the plasma gets colder because of evaporation of water. Subsequently, the small particles may get agglomerated by sintering with other particles and liquid gets evaporated. The agglomeration progresses until an impact with the substrate. This is confirmed by the aspect of surface of the coatings sprayed using greater spray distance, which visualize some agglomerates (Fig. 2a). As the atmosphere around solid precursors contains a lot of vapors of water, the solidification of small particles in-flight before the impact with the substrate is possible. Anatase has lower interfacial energy between liquid and solid  $\text{TiO}_2$  and this phase is likely to nucleate firstly (Ref 26). Moreover, the cooling of a precursor in-flight is very rapid and anatase is likely to be formed in its entire volume because of their small size. An increase of anatase phase fraction with the spray distance can be attributed to the increasing number of solidified particles arriving on the substrate. The small particles being molten at impact with substrate nucleates as anatase but this phase can transform back to rutile on cooling of the coating. This transformation is even more likely for larger agglomerates due to the larger quantity of heat of fusion

liberated and lower cooling rate. As the size of anatase and rutile crystals, being about 100 nm is comparable to the size of small solid particles used in suspension formulation, it is reasonable to suppose that precursors are entirely rutile or entirely anatase. The anatase-precursors are generated in-flight and rutile-solids are unmelted ones and those which transform back from anatase-solids when the coating cools down. The ability to obtain anatase in suspension sprayed coatings is useful in their application in photocatalysis. The effect, discovered by Fujishima and Honda (Ref 27), occurs in the presence of  $\text{TiO}_2$ , water and air. The mechanism of photocatalysis applied for the decomposition of pesticides pollutants in water has been explained in Ref 28. The effect of photocatalysis is enhanced when  $\text{TiO}_2$  is crystallized as anatase. Suspension of  $\text{TiO}_2$  was used to deposited coatings tested to decompose different pollutant, for example:

- arc plasma spraying was used to decompose NO and  $\text{NO}_x$  contained in air (Ref 29);
- induction plasma spraying was applied to decompose 4-chlorophenol (Ref 30);
- high-velocity oxy-fuel spraying was used to degrade acetaldehyde in air (Ref 31).

The mechanical properties were studied in Ref 32 by the use of scratch test. The experiments were realized using a statistical design and the critical load was found to be in the range of 10 to 17 N. The load was depending mainly on the spray distance. The scratch hardness of the coatings was in the range of  $HS_L = 0.5\text{--}0.8$  GPa. The impedance spectroscopy measurements were carried out at high temperature in order to confirm the microstructure investigations. The results were interpreted in terms of coating microstructure and technology. As far as the microstructure is concerned, the analysis of equivalent circuits of the coatings indicates the presence of a low conducting, dielectric part, corresponding to rutile and anatase and a well conducting part, which corresponds to Magnéli phases. The influence of spray technology on equivalent circuits is discussed in more detail in Ref 33. Electron emission of suspension sprayed coatings has been studied in Ref 6 and 7. It was found that the coatings acted as composite field electron emitter according to the Forbes model. The obtained emission characteristics prove great impact of conditioning time on the maximum emission current. The resulted maximum emission current ranged from 230 to 400 mA depending on the suspension formulation which makes the coatings applicable for practical vacuum electronic devices.

### 3.2 HA Coatings

The initial idea of suspension spraying of hydroxyapatite comes from Sherbrooke University of Canada and the coatings were deposited using induction plasma (Ref 34). The technology has been recently taken over in Ecole Nationale Supérieure de Chimie de Lille on France with the use of arc plasma. The morphology of typical arc plasma sprayed coating obtained using alcohol with water

suspension HA and internal continuous stream injector is shown in Fig. 5. Some areas contain the grains which are agglomerated and molten (see right side of Fig. 5b). Some others, visible in the left side of Fig. 5(b), remain small and do not seem to be molten. Consequently, the coatings have *two zones microstructure* (Ref 35). The HA powder used to formulate the suspension was synthesized in the laboratory in the way described in Ref 36, 37. The XRD is shown in Fig. 6. Suspension plasma sprayed HA coatings included the following phases: HA,  $\alpha$ -TCP,  $\beta$ -TCP, and amorphous phase (ACP). The phase diagram allows, to a degree, predicting phenomena at flight of HA particles. The formation of amorphous calcium phosphates (ACP) can be attributed to the rapid cooling of melt. Similarly,  $\alpha$ -TCP formed on heating of HA and their presence in the coatings was explained at spraying of large particles by freezing of these phases at impact with the substrate (or previously deposited coating) (Ref 19). Finally, the presence of HA can be explained by the fact that some particles, or their parts, remain unheated or heated due to

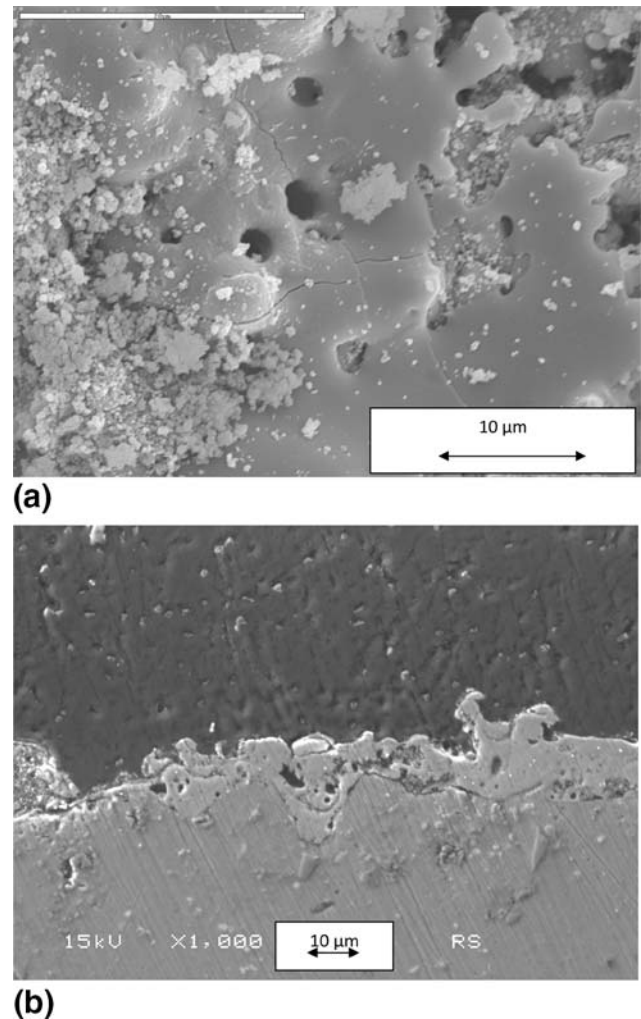


**Fig. 5** SEM (secondary electrons) of surface (a) and cross section (b) of suspension plasma sprayed HA coatings with internal continuous stream injector (Ref 27)

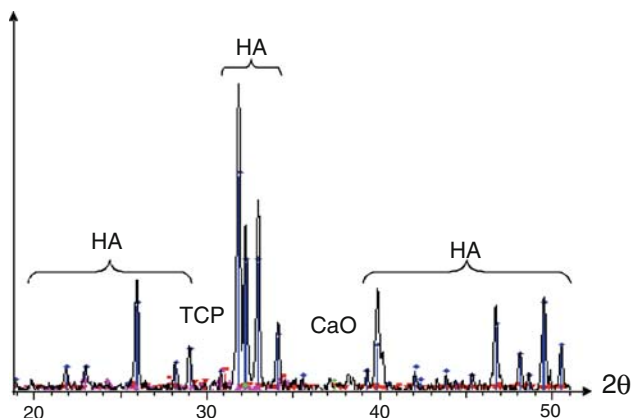


**Fig. 6** X-ray diagram of HA suspension sprayed coatings (Ref 28)

the temperatures below the temperature of phase transformation to  $\alpha$ -TCP and TTCP. The presence of  $\beta$ -TCP is unusual and the phase was not observed when sprayed the same HA powder having coarse particles in water and/or onto the substrate (Ref 21). The possible explanation is related to the small size of powder particles. The particles are a solid part of a water solution being injected into plasma jet. The stream of suspension is injected into plasma jet. It is possible that the stream was not injected perfectly in the middle of plasma jet and could have remained on the periphery of the plasma jet and the fine particles inside get only heated without melting. If the jet was injected into the hot temperature region of plasma jet, the droplets of liquid were accelerated in the plasma jet and disintegrated into smaller droplets. Simultaneously, water boiled and got evaporated. The temperature of some fine particles remained on the periphery of the plasma jet and may be greater than that of the transformation temperature of HA into  $\alpha$ -TCP.  $\beta$ -TCP, in turn, could have been formed from  $\alpha$ -TCP on cooling down. Similarly, CaO could have transformed from TTCP which is not detectable in the coating. The cooling of particles being on the periphery of the jet is less intensive than that being in the centre of the jet making possible such transformations. The mechanical properties of HA coatings were tested with the scratch test. The suspension plasma sprayed coatings on Ti substrate needs a critical load of about 12.3 N to be denuded. The scratch hardness was in the range  $HS_L = 0.7\text{--}1.2$  GPa. The dielectric strength of the coatings, tested at dc, ranged from 50 to 230 kV/cm (Ref 38).

### 3.3 Multilayer Composites $\text{TiO}_2$ and HA

The handling of suspensions using a couple of peristaltic pumps makes it easy to control their feed rate and to mix them. This opens a way to design the multilayer composites. A practical realization of the idea was realized by controlling the feed rate of  $\text{TiO}_2$  and HA suspension (Ref 13). Consequently, the multilayer coating with a gradient of chemical composition which started with  $\text{TiO}_2$

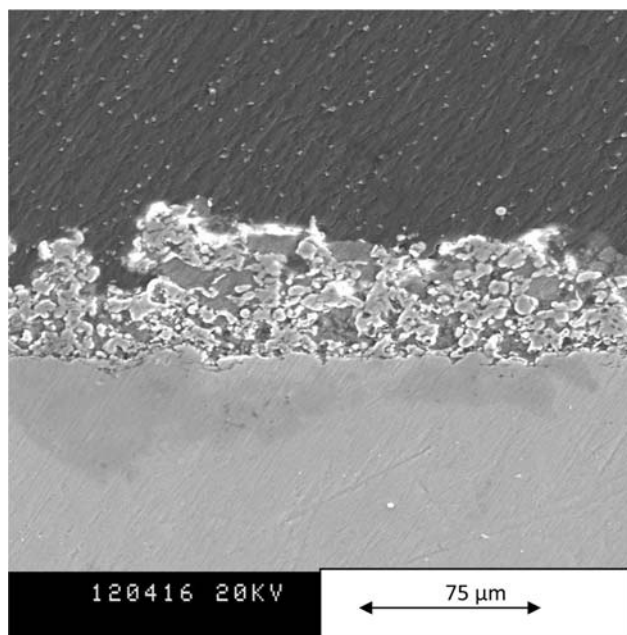


**Fig. 7** SEM micrograph (secondary electrons) of cross section of multilayer  $\text{TiO}_2$  and HA coating with gradient of chemical composition sprayed using atomizer injector (Ref 11)

at the interface with Ti substrate and finished with HA at the coating surface was achieved (Fig. 7).

## 4. Conclusions

This paper describes the studies on  $\text{TiO}_2$ ,  $\text{Ca}_5(\text{PO}_4)_3\text{OH}$  (HA) and their composite multilayer coatings onto stainless steel, titanium and aluminum substrate using suspension plasma spraying. The suspensions were formulated with the use of fine commercial  $\text{TiO}_2$  pigment crystallized as rutile and HA milled from commercial spray-dried powder or synthesized from calcium nitrate and ammonium phosphate in an optimized reaction. Two types of liquid feeders were applied: mechanical and pneumatic. The injection of suspension to the plasma jet was studied carefully with the use of an atomizer injector or a continuous stream one. The sprayed deposits were submitted to the phase analysis by the use of x-ray diffraction. The content of anatase and rutile was calculated in the titanium oxide deposits as well as the content of the decomposition phases in the hydroxyapatite ones. The micro-Raman spectroscopy was used to visualize the area of appearance of some phases. Scratch test enabled to characterize the adhesion of the deposits, their micro-hardness and friction coefficient. The electric properties including electron emission, impedance spectroscopy, dielectric properties of some coatings were equally tested. Several properties of the coatings were expressed by the deposition variables by the use of statistical regression equations. The present research work is being carried out with the use internal continuous stream injector fed by the

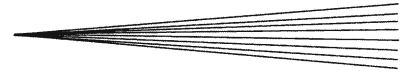
pneumatic suspension feeder. Such injection seems to be the way to reduce the porosity of suspension sprayed coatings.

## Acknowledgments

The contributions in the research of Drs. Rafal Tomaszek (Bodycote), Jacky Laureyns (University of Lille 1), Léon Gengembre (University of Lille 1) and Zbigniew Znamirowski (Wroclaw University of Technology) are warmly acknowledged.

## References

1. P. Fauchais and G. Montavon, Latest Developments in Suspension and Liquid Precursor Thermal Spraying, *Thermal Spray 2009: Proceedings of the International Thermal Spray Conference*, B.R. Marple, M.M. Hyland, Y.-C. Lau, C.-J. Li, R.S. Lima, and G. Montavon, Ed., p 136-149
2. L. Pawlowski, Suspension and Solution Thermal Spray Coatings, *Surf. Coat. Technol.*, 2009, **203**, p 2807-2829
3. G.K. Mor, O.K. Varghese, M. Paulose, K.G. Ong, and C.A. Grimes, Fabrication of Hydrogen Sensors with Transparent Titanium Oxide Nanotube-Array Thin Films as Sensing Elements, *Thin Solid Films*, 2006, **496**(1), p 42-48
4. L. Castaneda, Effects of Palladium Coatings on Oxygen Sensors of Titanium Dioxide Thin Films, *Mater. Sci. Eng. B*, 2007, **139**(2-3), p 149-154
5. F. Ye and A. Ohmori, The Photocatalytic Activity and Photo-Absorption of Plasma Sprayed  $\text{TiO}_2\text{-Fe}_3\text{O}_4$  Binary Oxide Coatings, *Surf. Coat. Technol.*, 2002, **160**, p 62-67
6. R. Tomaszek, Z. Znamirowski, L. Pawlowski, and A. Wojnakowski, Temperature Behaviour of Titania Emitters Realized by Suspension Plasma Spraying, *Surf. Coat. Technol.*, 2006, **201**, p 2099-2102
7. R. Tomaszek, Z. Znamirowski, L. Pawlowski, and J. Zdanowski, Effect of Conditioning on Field Electron Emission of Suspension Plasma Sprayed  $\text{TiO}_2$  Coatings, *Vacuum*, 2007, **81**, p 1278-1282
8. T. Moskalewicz, A. Czyska-Filemonowicz, and A.R. Boccacini, Microstructure of Nanocrystalline  $\text{TiO}_2$  Films Produced by Electrophoretic Deposition on Ti-6Al-7Nb Alloy, *Surf. Coat. Technol.*, 2007, **201**, p 7467-7471
9. L.-M. Berger, Titanium Oxide—New Opportunities for an Established Coating Material, *ITSC 2004, Thermal Spray 2004: Advances in Technology and Application*, May 10-12, 2004 (Osaka, Japan), Conference Proceedings on CD-Rom, ASM International, DVS-Verlag, Düsseldorf, Germany, ISBN 3-87155-792-7
10. A. Killinger, M. Kuhn, and R. Gadow, High-Velocity Suspension Flame Spraying (HVSFS), a New Approach for Spraying Nanoparticles with Hypersonic Speed, *Surf. Coat. Technol.*, 2006, **201**, p 1922-1930
11. F.-L. Toma, G. Bertrand, D. Klein, C. Coddet, and C. Meunier, Photocatalytic Decomposition of Nitrogen Oxides Over  $\text{TiO}_2$  Coatings Elaborated by Liquid Feedstock Plasma Spraying, *ITSC 2005*, May 2-4 (Basel, Switzerland), Conference Proceedings on CD-Rom, DVS-Verlag, Düsseldorf, Germany, ISBN 3-87155-793-7
12. R. Tomaszek, L. Pawlowski, L. Gengembre, J. Laureyns, Z. Znamirowski, and J. Zdanowski, Microstructural Characterization of Plasma Sprayed  $\text{TiO}_2$  Functional Coating with Gradient of Crystal Grain Size, *Surf. Coat. Technol.*, 2006, **201**, p 45-56
13. R. Tomaszek, L. Pawlowski, L. Gengembre, J. Laureyns, and A. Le Maguer, Microstructure of Suspension Plasma Sprayed Multilayer Coatings of Hydroxyapatite and Titanium Oxide, *Surf. Coat. Technol.*, 2007, **201**, p 7432-7440
14. L. Sun, C.C. Berndt, K.A. Gross, and A. Kucuk, Material Fundamentals and Clinical Performance of Plasma-Sprayed Hydroxyapatite Coatings: A Review, *J. Biomed. Mater. Res. (Appl. Biomater.)*, 2001, **58**, p 570-592
15. J.L. Lee, L. Roubfar, and O.R. Beirne, Survival of Hydroxyapatite-Coated Implants: A Meta-Analytic Review, *J. Oral Maxillofac. Surg.*, 2000, **58**, p 1372-1379
16. M. Ogiso, Reassessment of Long Term Use of Dense HA as a Dental Implant: Case Report, *J. Biomed. Mater. Res. (Appl. Biomater.)*, 1998, **43**, p 318-320
17. W. Suchanek, M. Yashima, M. Kakihana, and M. Yoshimura, Processing and Mechanical Properties of Hydroxyapatite Reinforced with Hydroxyapatite Whiskers, *Biomaterials*, 1996, **17**, p 1715-1723
18. L. Pawlowski, *The Science and Engineering of Thermal Spray Coating*, 2nd ed., Wiley, Chichester, UK, 2008
19. S. Dyshlovenko, B. Pateyron, L. Pawlowski, and D. Murano, Numerical Simulation of Hydroxyapatite Powder Behaviour in Plasma Jet, *Surf. Coat. Technol.*, 2004, **179**, p 110-117 and its corrigendum in *Surf. Coat. Technol.*, **187**, p 408-409
20. J. Weng, Q. Liu, J.G.C. Wolke, and K. de Groot, Formation and Characteristics of the Apatite Layer on Plasma-Sprayed Hydroxylapatite Coatings in Simulated Body Fluid, *J. Mater. Sci. Lett.*, 1997, **16**, p 335-337
21. S. Dyshlovenko, L. Pawlowski, P. Roussel, D. Murano, and A. Le Maguer, Relationship Between Plasma Spray Operational Parameters and Microstructure of Hydroxyapatite Coatings and Powder Particles Sprayed into Water, *Surf. Coat. Technol.*, 2006, **200**, p 3845-3855
22. V. Deram, C. Minichiello, R.-N. Vannier, A. Le Maguer, L. Pawlowski, and D. Murano, Microstructural Characterizations of Plasma Sprayed Hydroxyapatite Coatings, *Surf. Coat. Technol.*, 2003, **166**(2-3), p 153-159
23. H. Podlesak, L. Pawlowski, J. Laureyns, R. Jaworski, and T. Lampke, Advanced Microstructural Study of Suspension Plasma Sprayed Titanium Oxide Coatings, *Surf. Coat. Technol.*, 2008, **202**, p 3723-3731
24. R. Jaworski, L. Pawlowski, F. Roudet, S. Kozerski, and A. Le Maguer, Influence of Suspension Plasma Spraying Process Parameters on  $\text{TiO}_2$  Coatings Microstructure, *J. Therm. Spray Technol.*, 2008, **17**(1), p 73-81
25. K. Masters, *Spray Drying Handbook*, 4th ed., George Godwin, London, UK, 1985
26. Y. Li and T. Ishigaki, Thermodynamic Analysis of Nucleation of Anatase and Rutile from  $\text{TiO}_2$  Melt, *J. Cryst. Growth*, 2002, **242**, p 511-516
27. A. Fujishima and K. Honda, Electrochemical Photolysis of Water at a Semiconductor Electrode, *Nature*, 1972, **238**, p 37-38
28. J.-M. Herrmann and C. Guillard, Photocatalytic Degradation of Pesticides in Agricultural Used Water, *Compt. Rend. Acad. Sci. II C (Chem.)*, 2000, **3**(6), p 399-417
29. F.-L. Toma, G. Bertrand, S.O. Chwa, C. Meunier, D. Klein, and C. Coddet, Comparative Study on the Photocatalytic Decomposition of Nitrogen Oxides Using  $\text{TiO}_2$  Coatings Prepared by Conventional Plasma Spraying and Suspension Plasma Spraying, *Surf. Coat. Technol.*, 2006, **200**, p 5855-5862
30. I. Burlacov, J. Jirkovsky, M. Müller, and R.B. Heimann, Induction Plasma-Sprayed Photocatalytically Active Titania Coatings and Their Characterisation by Micro-Raman Spectroscopy, *Surf. Coat. Technol.*, 2006, **201**(1-2), p 255-264
31. F.-L. Toma, L.M. Berger, D. Jacquet, D. Wicky, I. Villaluenga, Y.R. de Miguel, and J.S. Lindeløv, Comparative Study on the Photocatalytic Behaviour of Titanium Oxide Thermal Sprayed Coatings from Powders and Suspensions, *Surf. Coat. Technol.*, 2009, **203**(15), p 2150-2156
32. R. Jaworski, L. Pawlowski, F. Roudet, S. Kozerski, and F. Petit, Characterization of Mechanical Properties of Suspension Plasma Sprayed  $\text{TiO}_2$  Coatings Using Scratch Test, *Surf. Coat. Technol.*, 2008, **202**, p 2544-2553
33. R. Tomaszek, K. Nitsch, L. Pawlowski, Z. Znamirowski, and M. Brylak, Impedance Spectroscopy of Suspension Plasma Sprayed Titania Coatings, *Surf. Coat. Technol.*, 2006, **201**, p 1930-1934
34. E. Bouyer, F. Gitzhofer, and M.I. Boulos, The Suspension Plasma Spraying of Bioceramics by Induction Plasma, *JOM*, 1997, **49**(2), p 58-62



35. S. Kozerski, L. Pawlowski, R. Jaworski, F. Roudet, and F. Petit, Two Zone Microstructure of Suspension Plasma Sprayed Hydroxyapatite Coatings, *Surf. Coat. Technol.*, 2009. doi:[10.1016/j.surfcoat.2009.09.020](https://doi.org/10.1016/j.surfcoat.2009.09.020)
36. R. Jaworski, C. Pierlot, L. Pawlowski, M. Bigan, and M. Martel, Design of the Synthesis of Fine HA Powder for Suspension Plasma Spraying, *Surf. Coat. Technol.*, 2009, **203**, p 2092-2097
37. R. Jaworski, C. Pierlot, L. Pawlowski, M. Bigan, and M. Quivrin, Synthesis and Preliminary Tests of Suspension Plasma Spraying of Fine Hydroxyapatite Powder, *J. Therm. Spray Technol.*, 2008, **17**(5-6), p 679-684
38. R.J. Jaworski, C. Pierlot, R. Tomaszek, L. Pawlowski, and Z. Znamirowski, Optimization of Dielectric Properties of Suspension Plasma Sprayed Hydroxyapatite Coatings, *Mat.-wiss.u. Werkstofftech.*, 2007, **38**(2), p 125-130